Computational and Experimental Study to Evaluate the Resonance Condition of the Standing Wave Acoustic Levitation System

Saurabh YADAV
Indian Institute of Technology Mandi, India, saurabh16yadav@gmail.com

Arpan GUPTA
Indian Institute of Technology Mandi, India, agupta@iitmandi.ac.in

Abstract: - Acoustic levitation is a technique for non-contact processing and hence very useful in different areas like chemical reactions of highly reactive substances. Resonance is the key reason for the Standing wave acoustic levitation system and depends on the right distance between the driver and the reflector surfaces. In this paper, the finite difference method is used to calculate the distance between the driver and reflector surfaces for resonance phenomenon. Two different computational domains- 1D and 2D geometry of the levitation system are considered for the study. The finite difference results are supplemented by 2D axisymmetric Finite Element simulation (implemented in COMSOL Multiphysics) to find the resonance condition. To validate the numerical results, an experimental setup is prepared and eighth resonance mode is considered. The distance between the driver surface and the reflector surface is calculated for eighth resonance mode from finite difference method, COMSOL Multiphysics and experimental method. It is found that the numerical results are in good agreement with the experimental result. Thus, even the 1D and 2D finite difference code can accurately predict the distance requirement for acoustic levitation system.

Keywords: - Finite difference method, Acoustic levitation, Resonance, Standing wave acoustic levitation.

1. INTRODUCTION

Acoustic levitation is an impressive technique, which is used to levitate the particles/objects freely in a medium. The acoustic radiation pressure is used to trap the object and levitate with no contact. Solid particles as well as the liquid droplets of different substances can be levitated freely. The standing wave acoustic levitation has been used to calculate the different properties, like density, surface tension, sound velocity, viscosity etc., of the liquids at a normal temperature [1]–[4] as well as of the supercooled liquids [5], [6]. Studying the melting/ solidification of solids using the acoustic levitation can also help avoid the sample's contamination during the process. It can also improve the properties by uniform solidification from all sides.

The melting and solidification of acoustically levitated commercial-grade succinonitrile have been studied [7]. The acoustic levitation technique is also instrumental in handling the tiny components in micro-assembly [8]. This levitation technique can be used to levitate the heaviest solid, Iridium (having the density of 22.6 g.m-3) as well as the heaviest liquid, Mercury (having the density of 13.6 g.m-3) on the earth [9]. Not only the solid particles or the liquid drops of the matters, some of the small living creatures like the ant, ladybug and young fish are also successfully levitated in the air using standing wave acoustic levitation [10].

Different studies have been performed to study the different standing wave acoustic levitation system parameters and tried to maximize the levitation force of the acoustic levitation system [11]–[14].

Barmatz et al. developed an economical technique to control the object's orientation levitating between the standing wave acoustic levitation system [15].

Standing wave acoustic levitation system consists of a driver and a reflector. At resonance, there is a standing wave formed between the driver and the reflector. Particles can be levitated stably near the pressure nodes of the standing wave. The distance between the driver surface and the reflector (or driver, if the system has the driver at both ends) surface is vital to obtain the resonance condition, which leads to the formation of the standing wave.

Different methods, like Finite element method and Matrix method, have been used to study the standing wave acoustic levitation system [16]–[19]. In this paper, the Finite difference method is used to determine the levitation system's resonance condition, which has a driver at one end and the reflector at the other. The finite difference results are also compared with the simulation software COMSOL Multiphysics result as well as the experimental result.

2. NUMERICAL MODELING

2.1. Finite Difference Modeling

From the equation of state, continuity equation and the force equation, the acoustic wave equation can be derived. General mathematical expression for acoustic wave equation can be represented by Eq. (1) [20].

$$\frac{\partial^2 p}{\partial t^2} = c^2 \nabla^2 p \tag{1}$$

where p and c are the sound pressure amplitude and speed of sound, respectively.

Using the method of separation of variables, the partial differential equation, Eq. (1) can be reduced to two ordinary differential equations. The separated ordinary differential equation in space coordinates represents the time-independent harmonic wave equation. It is also known as the Helmholtz equation and can be represented by Eq. (2).

$$\nabla^2 p + k^2 p = 0 \tag{2}$$

where $k = \frac{\omega}{c}$, and known as the wavenumber. ω is the angular frequency. The differential operator can be expressed as

For 1D:

$$\nabla^2 = \frac{\partial^2}{\partial z^2}$$

For 2D:

$$\nabla^2 = \frac{\partial^2}{\partial x^2} + \frac{\partial^2}{\partial z^2}$$

The derivative can be approximated by the central difference formula of the finite difference method. After approximation, the Eq. (2) can be represented as-

For 1D:

$$\frac{p_{k+1} - 2p_k + p_{k-1}}{\Delta h_z^{\ 2}} + k^2 p_k = 0 \tag{3}$$

For 2D:

$$\frac{p_k^{i+1} - 2p_k^i + p_k^{i-1}}{\Delta h_x^{\ 2}} + \frac{p_{k+1}^i - 2p_k^i + p_{k-1}^i}{\Delta h_z^{\ 2}} + k^2 p_k^i = 0 \tag{4}$$

where i and k denote the discretization index in x and z, respectively. Δh_x and Δh_z are the step size in x and z direction, respectively.

The boundary conditions used in the model are sound hard boundary condition and non-reflecting boundary condition. The simplified mathematical expressions for sound hard boundary condition and non-reflecting boundary condition are represented by the Eq. (5) and Eq. (6), respectively.

$$\nabla p = 0 \tag{5}$$

$$\nabla p + kp = 0 \tag{6}$$

Approximating these boundary condition mathematical expressions using the central difference formula, Eq. (5) and Eq. (6) can be represented by the following expressions-

For 1D:

Sound hard boundary condition-

$$\left.\begin{aligned} &\frac{p_{k+1} - p_{k-1}}{2\Delta h_z} = 0 \\ &\text{or} \\ &p_{k+1} = p_{k-1} \end{aligned}\right\} \tag{7}$$

For 2D:

Sound hard boundary condition-

$$\left.\begin{aligned} &\text{For x-direction:} \\ &\frac{p_k^{i+1} - p_k^{i-1}}{2\Delta h_x} = 0 \\ &\text{or} \\ &p_k^{i+1} = p_k^{i-1} \\ &\text{For z-direction:} \\ &\frac{p_{k+1}^i - p_{k-1}^i}{2\Delta h_z} = 0 \\ &\text{or} \\ &p_{k+1}^i = p_{k-1}^i \end{aligned}\right\} \tag{8}$$

Non-reflecting boundary condition-

$$\left.\begin{aligned} &\text{For x-direction:} \\ &\frac{p_k^{i+1} - p_k^{i-1}}{2\Delta h_x} + kp_k^i = 0 \\ &\text{or} \\ &p_k^{i+1} - p_k^{i-1} = -2\Delta h_x k p_k^i \\ &\text{For z-direction:} \\ &\frac{p_{k+1}^i - p_{k-1}^i}{2\Delta h_z} + kp_k^i = 0 \\ &\text{or} \\ &p_{k+1}^i - p_{k-1}^i = -2\Delta h_z k p_k^i \end{aligned}\right\} \tag{9}$$

2.2. Geometry for Numerical Study

The standing wave acoustic levitation system can have a driver at one end and a reflector at other or the drivers at both ends. For the finite difference study, the levitation system is considered with a sound source at the bottom end and a reflector at the top end. The sound hard boundary condition is provided at the top boundary to make it work as a reflector.

A harmonic input pressure of magnitude 20 Pa is provided at the sound source which generates the sound wave of 40.305 kHz. The acoustic wave equation (Helmholtz equation) is solved for 1D as well as the 2D geometry to find out the resonance condition of the acoustic levitator.

For 2D geometry, the axisymmetric model is used. The radius of the driver and the air domain are considered as 22.5 mm and 30 mm, respectively. The sound source provided at the bottom boundary is shown with the blue line in Fig. 1(a).

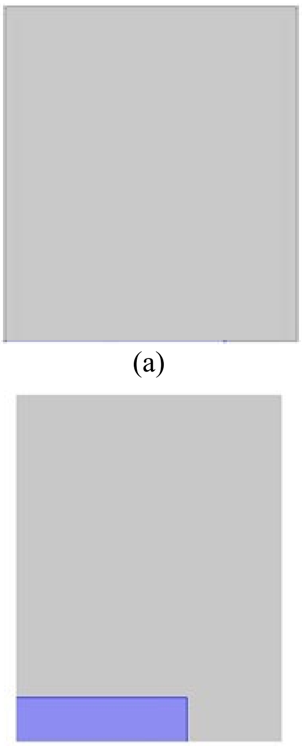

(a)

(b)

Figure 1. Geometry of the standing wave acoustic levitation system (a) for finite difference study and (b) for COMSOL Multiphysics study

For the numerical study using the Finite Element Method (FEM) implemented in COMSOL Multiphysics, the 2D axisymmetric model is used. The standing wave acoustic levitator's geometry for the COMSOL Multiphysics is designed to replicate experiment more closely.

The radius of the driver and the air domain is 22.5 mm and 30 mm respectively, as shown in the Fig. 1(b).

For the COMSOL study, the acoustic structure interaction is used. The harmonic excitation with some displacement amplitude is provided to the driver. Due to the vibration of the driver, the sound waves are generated. In Fig. 1(a) and 1(b), the grey part is the air domain, and the blue part is the driver. The top boundary of the air domain is provided with the sound hard boundary condition. So, it works as the reflector.

Bottom boundary (right side of the driver) is also provided with the sound hard boundary condition. For the finite difference study as well as the COMSOL Multiphysics study, the axisymmetric model is used. So, the left side boundary of the air domain is provided with the sound hard boundary condition.

The right-side boundary of the air domain is provided with the non-reflecting boundary condition. So that no sound radiation is coming back from the right boundary.

2.3. Experimental Setup

Firstly, the exact working frequency or the resonance frequency of the ultrasonic transducer is calculated experimentally (which comes to 40.305 kHz). The circuit diagram, shown in Fig. 2(a), is used to calculate the resonance frequency of the transducer experimentally.

The channel 1 of the oscilloscope is connected to the output of the signal generator and gives the voltage applied (5 V). NI virtual bench function generator is used as the signal generator.

The channel 2 is connected to the 100 ohms register which gives the current flowing through the circuit. To find out the resonance frequency of the transducer, the frequency of the signal is varied slowly. The frequency, at which the measured current and the voltage are in phase and the current drawn is maximum, is the resonance frequency of the transducer.

Fig. 2(b) shows the complete experimental setup with ultrasonic transducer, which is used as the driver for the standing wave acoustic levitation system.

The bottom part of the driver is fixed with the help of the driver holder. The driver holder is placed at the top of the tripod. The acrylic sheet of 6 mm thickness is used as the reflector. The distance between the driver surface and the reflector surface is varied with the help of the tripod.

The driver is excited with the signal of 40.305 kHz (which is the resonance frequency of the ultrasonic transducer/driver).

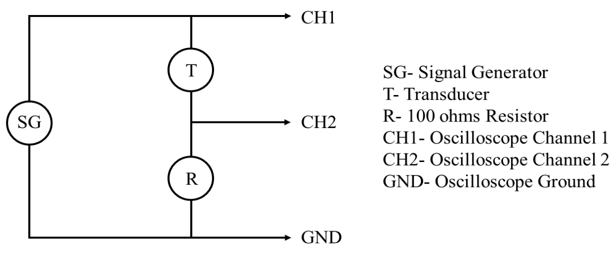

(a)

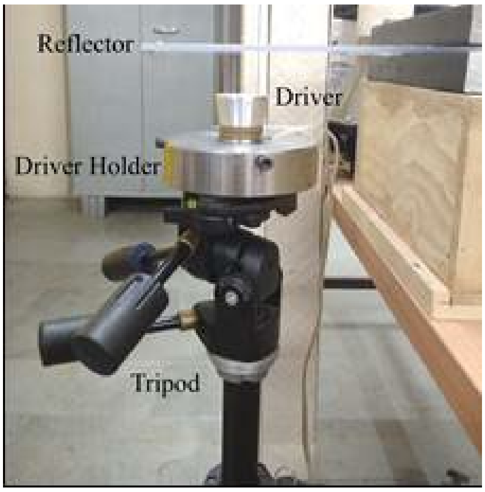

(b)

Figure 2. (a) Circuit diagram to calculate the resonance frequency of the driver/transducer, (b) Experimental setup of standing wave acoustic levitation system

2.4. Convergence Study

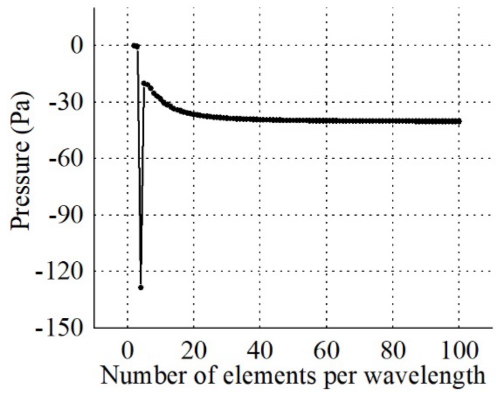

(a)

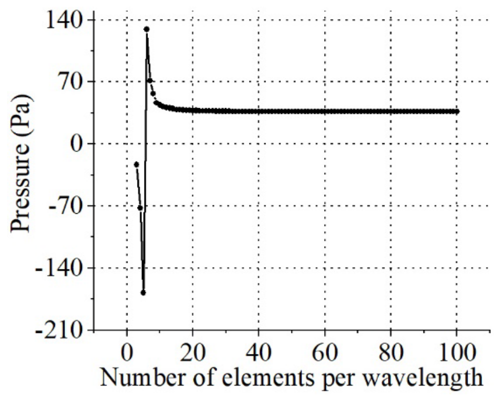

(b)

Figure 3. Convergence plot for (a) 1D and (b) 2D geometry

The acoustic wave equation is solved for 1D as well as 2D using finite difference method implemented on MATLAB software. The convergence study is performed to find out the optimum element size for geometry mesh. Fig. 3(a) and 3(b) shows the convergence plot for 1D and 2D geometry, respectively.

The solution is almost converged at the 50 elements per wavelength for both the cases. So, the element size is considered as λ/50 (λ is wavelength corresponding to the 40.305 kHz).

3. RESULTS AND DISCUSSION

In this study, the right air gap for the eighth resonance mode of the standing wave acoustic levitator is calculated. The excitation frequency of the driver is considered as 40.305 kHz. Firstly, the resonance condition is calculated for 1D and 2D geometry using finite difference method.

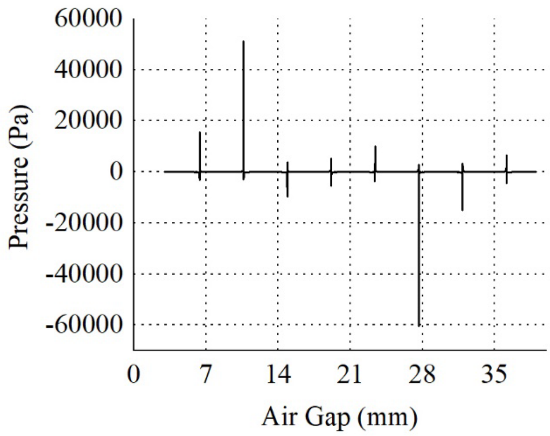

(a)

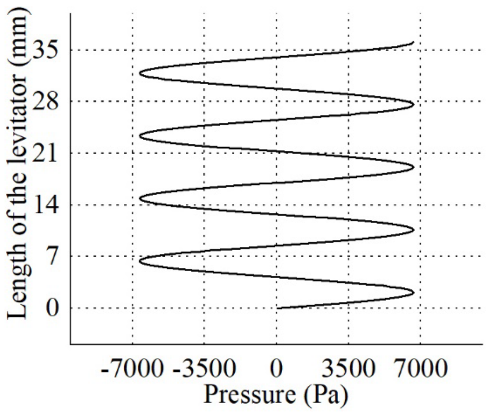

(b)

Figure 4. Using the finite difference method for 1D model, (a) First eight resonance modes and (b) Pressure profile corresponding to the eighth resonance mode

The sound source is considered at the bottom, and the reflector is considered at the top. At resonance, the standing wave is formed between the sound source and the reflector surface. For 1D, the acoustic pressure is calculated at the reflector surface (there is pressure anti-node near reflector surface at resonance). At resonance, the acoustic pressure fluctuation is maximum at pressure antinode. Fig. 4(a) shows the plot between acoustic pressure and the air gap between the driver and the reflector surface. First eight resonance modes are shown in Fig. 4(a). The eighth resonance mode is selected to compare the different numerical models as well as the experiment. The air gap corresponding to the eighth resonance mode is calculated as 36.14 mm. Fig. 4(b) shows the pressure profile of the 1D case at eighth resonance mode.

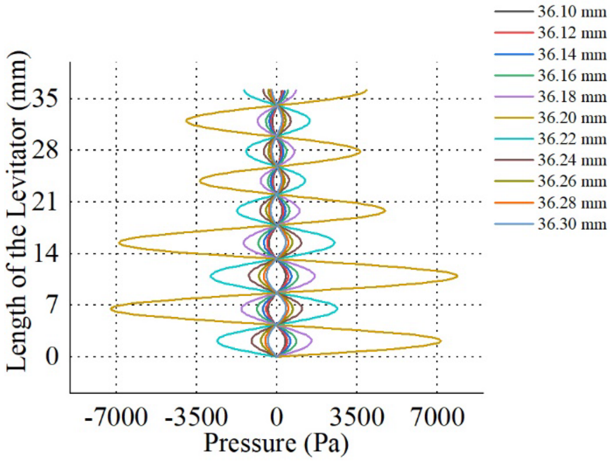

(a)

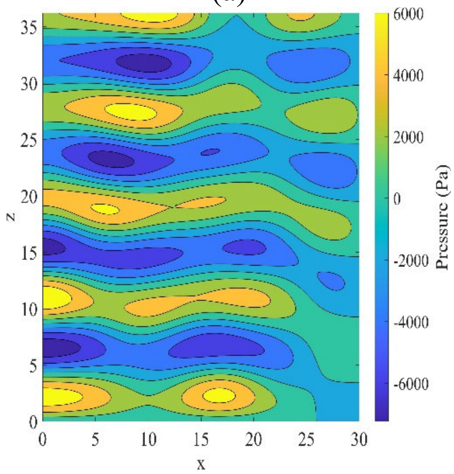

(b)

Figure 5. (a) Pressure value along the central axis of the levitator for different air gaps, (b) Pressure profile at eighth resonance mode (36.20 mm)

For 2D using finite difference, the acoustic pressure is calculated at the standing wave acoustic levitation system's central axis for the resonance conditions. At resonance, the pressure fluctuations are maximum at pressure anti-nodes and minimum at pressure nodes. The resonance condition corresponding to the eighth resonance mode is calculated. Fig. 5 (a) shows the acoustic pressure value along the central axis of the 2D finite difference model of levitator (shown in Fig. 1(a)) for different length of the levitator (air gap between the driver and the reflector surfaces). The air gap corresponding to the eighth resonance mode is computed as 36.20 mm. Figure 5(b) shows the axially symmetric (about x =0) pressure profile of the levitator at eighth resonance mode.

Further, the resonance condition corresponding to the eighth resonance mode for standing wave acoustic levitation system is calculated using 2D axisymmetric model of COMSOL Multiphysics. The acoustic structure interaction is used. The value of the air gap between the driver surface and the reflector surface is calculated as 34.35 mm, and the axis-symmetric pressure profile corresponding to the resonance condition is shown in Fig. 6(a). The air gap corresponding to the eighth resonance mode is also calculated experimentally to be 34.3 mm. Fig. 6(b) shows the standing wave acoustic levitation system at eighth resonance mode with small polystyrene balls levitating freely at the pressure nodes. The small polystyrene balls are of average diameter 3 mm and the average weight of 0.15 mg. As shown in Fig. 5(a), 5(b) and Fig. 6(a), there are eight pressure nodes with minimum pressure fluctuation. But there are seven polystyrene balls which are levitating in the experiment, as shown in Fig. 6(b). Due to the small hole in the transducer's surface, the polystyrene ball cannot be levitated near the eighth pressure node near the transducer.

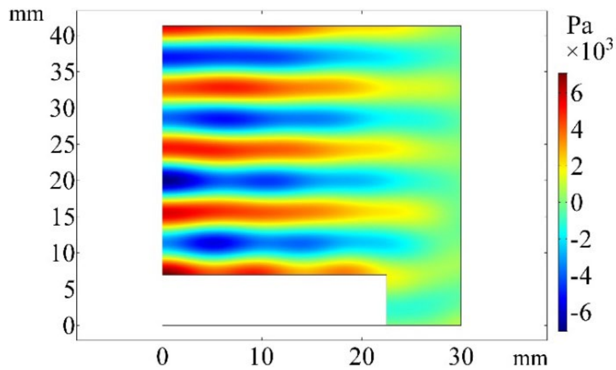

(a)

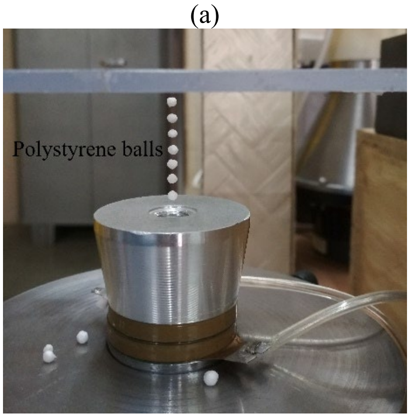

(b)

Figure 6. (a) Pressure profile at eighth resonance mode using COMSOL Multiphysics (b) Experimental setup with polystyrene balls levitating freely in the air

All the values, using different models for calculating air gap corresponding to the eighth resonance mode of the standing wave acoustic levitation system, are presented in Table 1.

Table 1. Comparison of results of different methods corresponding to the fourth resonance mode of standing wave acoustic levitation system

Finite Difference Results	1D	36.14 mm
	2D	36.20 mm
COMSOL Multiphysics Result		34.35 mm
Experimental Result		34.30 mm
% Error in finite difference w.r.t. Experimental Result	1D	5.36 %
	2D	5.54 %

4. CONCLUSIONS

In this paper, the resonance condition of the standing wave acoustic levitation system is studied. The finite difference method, finite element method (implemented on COMSOL Multiphysics), as well as the experimental method, are used for the study. The results (the value of the air gap between the driver and the reflector surfaces) corresponding to the eighth resonance mode are calculated and compared. Two different cases, 1D and 2D axisymmetric, are solved using the finite difference method. The air gap corresponding to the eighth resonance mode is found as 36.14 mm and 36.20 mm for 1D and 2D, respectively.

Further, the 2D axisymmetric model with acoustic structure interaction of COMSOL Multiphysics is used, and the value of the air gap corresponding to the eighth resonance mode is calculated as 34.35 mm. The experimental setup of the standing wave acoustic levitation system is prepared and used to obtain the air gap corresponding to the eighth resonance mode. The experimental value for the air gap is obtained as 34.30 mm. It is found that the COMSOL Multiphysics result and the experimental result are almost the same. The finite difference results are also in good agreement with the experimental result. One of the reasons for deviation in result can be the uniform pressure profile assumed in the finite difference study. However, the acoustic structure interaction in FEM captures the sound radiation pattern from a uniformly vibrating disk/diaphragm. Thus, the pressure profile generated by the transducer is more accurately represented in FEM study. Nonetheless, the margin of error between the methods used is less and provide us with simple yet robust tool for predicting resonance condition in acoustic levitation system.

REFERENCES

[1] Y. Tian, R. G. Holt, and R. E. Apfel, “A new method for measuring liquid surface tension with acoustic levitation,” Rev. Sci. Instrum., vol. 66, no. 5, pp. 3349–3354, 1995.

[2] E. H. Trinh and C. J. Hsu, “Acoustic levitation methods for density measurements,” J. Acoust. Soc. Am., vol. 80, no. 6, pp. 1757–1761, 1986.

[3] R. E. Apfel, “Technique for measuring the adiabatic compressibility, density, and sound speed of submicroliter liquid samples,” J. Acoust. Soc. Am., vol. 59, no. 2, pp. 339–343, 1976.

[4] J. Kremer, A. Kilzer, and M. Petermann, “Simultaneous measurement of surface tension and viscosity using freely decaying oscillations of acoustically levitated droplets,” Rev. Sci. Instrum., vol. 89, no. 1, p. 015109, 2018.

[5] E. H. Trinh and R. E. Apfel, “Sound velocity of supercooled water down to -33 ° C using acoustic levitation,” J. Chem. Phys., vol. 72, no. 12, pp. 6731–6735, 1980.

[6] E. H. Trinh and K. Ohsaka, “Measurement of density, sound velocity, surface tension, and viscosity of freely suspended supercooled liquids,” Int. J. Thermophys., vol. 16, no. 2, pp. 545–555, 1995.

[7] K. Ohsaka and E. H. Trinh, “Melting and solidification of acoustically levitated drops,” J. Cryst. Growth, vol. 96, pp. 973–978, 1989.

[8] V. Vandaele, P. Lambert, and A. Delchambre, “Non-contact handling in microassembly: Acoustical levitation,” Precis. Eng., vol. 29, pp. 491–505, 2005.

[9] W.-J. Xie, C. D. Cao, Y. J. Lü, and B.-B. Wei, “Levitation of iridium and liquid mercury by ultrasound,” Phys. Rev. Lett., vol. 89, no. 10, p. 104304, 2002.

[10] W.-J. Xie, C. D. Cao, Y. J. Lü, Z. Y. Hong, and B.-B. Wei, “Acoustic method for levitation of small living animals,” Appl. Phys. Lett., vol. 89, no. 21, p. 214102, 2006.

[11] S. Yadav and A. Gupta, “Maximization of Acoustic Levitating Force for a Single-Axis Acoustic Levitation System Using the Finite Element Method,” Chinese Phys. Lett., vol. 36, no. 3, p. 034302, 2019.

[12] W. J. Xie and B. Wei, “Parametric study of single-axis acoustic levitation,” Appl. Phys. Lett., vol. 79, no. 6, pp. 881–883, 2001.

[13] W. A. Oran, L. H. Berge, and H. W. Parker, “Parametric study of an acoustic levitation system,” Rev. Sci. Instrum., vol. 51, no. 5, pp. 626–631, 1980.

[14] S. Yadav and A. Gupta, “Parametric Study of Driver and Reflector of Single Axis Acoustic Levitator using Finite Element Method,” Acoust. Phys., vol. 66, no. 3, pp. 242–249, 2020.

[15] M. B. Barmatz, M. S. Gaspar, and E. H. Trinh, “Simplified rotation in acoustic levitation,” J. Acoust. Soc. Am., vol. 88, no. 6, pp. 2897–2897, 1990.

[16] H. Hatano, “Axisymmetric Analysis of a Tube-Type Acoustic Levita or by a Finite Element Method,” IEEE Trans. Ultrason. Ferroelectr. Freq. Control, vol. 41, no. 5, pp. 772–777, 1994.

[17] M. A. B. Andrade, F. Buiochi, and J. C. Adamowski, “Matrix Method for Acoustic Levitation Simulation,” IEEE Trans. Ultrason. Ferroelectr. Freq. Control, vol. 58, no. 8, pp. 1674–1683, 2011.

[18] M. A. B. Andrade, F. C. Buiochi, and J. Adamowski, “Finite element analysis and optimization of a single-axis acoustic levitator,” IEEE Trans. Ultrason. Ferroelectr. Freq. Control, vol. 57, no. 2, pp. 469–479, 2010.

[19] S. Yadav, and A. Gupta, “Finite Difference Study to Evaluate the Resonance Condition of the Standing Wave Acoustic Levitation System,” J. Vib. Eng. Technol. (2023).

[20] L. E. Kinsler, A. R. Frey, A. B. Coppens, and J. V. Sanders, Fundamentals of Acoustics, 4th Edi. John Wiley & Sons, Inc., 2000.